Inflammation Research (2024) 73:1223–1237
https://doi.org/10.1007/s00011-024-01894-5

ORIGINAL RESEARCH PAPER

Vistusertib improves pulmonary inflammation and fibrosis by modulating inflammatory/oxidative stress mediators via suppressing the mTOR signalling

Taslim B. Shaikh[1,2] · Yogesh Chandra[1] · Sai Balaji Andugulapati[1,2] · Ramakrishna Sistla[1,2]

Received: 25 March 2024 / Revised: 6 May 2024 / Accepted: 15 May 2024 / Published online: 24 May 2024
© The Author(s), under exclusive licence to Springer Nature Switzerland AG 2024

Abstract

Introduction Inflammation and oxidative stress are key factors in the development of pulmonary fibrosis (PF) by promoting the differentiation of fibroblasts through modulating various pathways including Wnt/β-catenin, TGF-β and mTOR signalling.

Objective and methods This study aimed to evaluate the effects and elucidate the mechanisms of vistusertib (VSB) in treating pulmonary inflammation/fibrosis, specifically by targeting the mTOR pathway using various in vitro and in vivo models.

Results Lipopolysaccharide (LPS)-induced inflammation model in macrophages (RAW 264.7), epithelial (BEAS-2B) and endothelial (HMVEC-L) cells revealed that treatment with VSB significantly reduced the IL-6, TNF-α, CCL2, and CCL7 expression. TGF-β induced differentiation was also significantly reduced upon VSB treatment in fibrotic cells (LL29 and DHLF). Further, bleomycin-induced inflammation and fibrosis models demonstrated that treatment with VSB significantly ameliorated the severe inflammation, and lung architectural distortion, by reducing the inflammatory markers expression/levels, inflammatory cells and oxidative stress indicators. Further, fibrosis model results exhibited that, VSB treatment significantly reduced the α-SMA, collagen and TGF-β expressions, improved the lung architecture and restored lung functions.

Conclusion Overall, this study uncovers the anti-inflammatory/anti-fibrotic effects of VSB by modulating the mTOR activation. Although VSB was tested for lung fibrosis, it can be tested for other fibrotic disorders to improve the patient's survival and quality of life.

Keywords mTOR inhibitor · Lung inflammatory cells · Lung fibroblast · Collagen deposition

Abbreviations

α-Sma	α-Smooth muscle actin
AECs	Alveolar epithelial cells
BMC	Bleomycin
CCL	Chemokine (CC-motif) ligand
CD	Cluster of differentiation
Col1a1	Collagen1alpha1
DEX	Dexamethasone
E-CAD	E-cadherin
ECM	Extracellular matrix
EMT	Epithelial-mesenchymal transition
FBS	Fetal bovine serum
FN1	Fibronectin 1
HO-1	Heme oxygenase-1
IFN	Interferon
IL	Interleukins
ILD	Interstitial lung diseases
IPF	Idiopathic pulmonary fibrosis
LPS	Lipopolysaccharide
MCP-1	Monocyte chemoattractant protein-1
Mmp	Matrix metalloproteinase
MPO	Myeloperoxidase

Communicated by Anatolii Kubyshkin.

✉ Sai Balaji Andugulapati
balaji@iict.res.in

✉ Ramakrishna Sistla
sistla@iict.res.in

[1] Division of Applied Biology, CSIR-Indian Institute of Chemical Technology, Hyderabad, Telangana 500 007, India

[2] Academy of Scientific and Innovative Research (AcSIR), Ghaziabad, Uttar Pradesh 201 002, India

mTOR	Mammalian target of Rapamycin
NE	Neutrophil elastase
NO	Nitric oxide
PBS	Phosphate buffer saline
PI3K	Phosphoinositide 3-kinase
PIFD	PirfenidoneROS: Reactive oxygen species
Tgf-β	Tumor growth factor-β
TNF	Tumor necrosis factor
VSB	Vistusertib

Introduction

Idiopathic pulmonary fibrosis (IPF), a type of interstitial lung anomaly, is considered a progressive, chronic, and fatal disease of unknown aetiology [1]. IPF remains a rare, orphan disease with global incidence and prevalence reported as 0.09–1.30 and 0.33–4.51 per 10,000 of the population respectively. Due to poor prognosis, the life expectancy of IPF patients is 2–5 years if left untreated. However, the approval of pirfenidone and nintedanib for the treatment of IPF was a significant milestone for the development of anti-fibrotic therapies [2, 3]. Although these agents decelerate disease progression, mortality remains largely unchanged which demands the identification of novel therapeutic approaches. To date, the pathophysiology of IPF has not been fully explored as it involves many different cellular, molecular, and immunological pathways for the development of the disease [4, 5]. The initiation of pulmonary fibrosis may be driven via microenvironmental injuries to alveolar epithelial cells (AECs). Microenvironmental injuries include a variety of intrinsic (age, genetic and gender) or extrinsic factors such as viral infection (COVID-19), cigarette smoke, or occupational exposures [6]. Pollutants and exogenous oxidants both promote the synthesis of oxidants and stimulate inflammatory cells, which release free radicals that result in damage to alveolar cells [7]. It has been postulated that alveolar epithelial cell apoptosis and elevated cellular oxidative stress are related to mitochondrial ROS production [8]. It has been stated that one of the main contributing factors to the aetiology of IPF is oxidant-antioxidant imbalances in the lower respiratory tract. Supporting that, myeloperoxidase and eosinophil cationic protein levels were shown to be elevated in IPF patients bronchoalveolar lavage fluid. Additionally, there is evidence associating enhanced myeloperoxidase with epithelial damage in IPF [9]. In lung injury conditions, AEC2 cells may stimulate an immune response to absolve the microenvironmental exposure. Once the insults are cleared, the inflammatory response fades away and the remaining AEC2s proliferate to heal injuries of the tissue, eventually leading to resolution [10]. On the other hand, if the insults continue, the injured epithelium and recruited inflammatory cells secrete a variety of signalling molecules including IL-4, IL-6, IL-1β, TNF-α, CTGF, PDGF, FGF, and TGF-β that modulate epithelial repair, promote fibroblast recruitment and myofibroblast activation, collagen synthesis, ECM deposition, apoptosis of AEC2 cells, EMT activation and ultimately fibrosis [11–13]. In addition to oxidative stress, EMT also plays a critical role in developing fibrosis. Although the source of myofibroblasts in IPF is debatable, it has been suggested that ATII (alveolar type II) cells that underwent EMT could serve as the origin of these cells in fibrosis [13]. Overall, oxidative stress, inflammation, and EMT are critical processes that activate one another and induce fibrosis, so addressing these events may be potential targets for treating IPF.

The TGF-β/SMAD signalling pathway plays a crucial role in the development of pulmonary fibrosis [14]. TGF-β-mediated AKT signalling, downstream of PI3K may further activate mTOR signalling. mTOR is a serine/threonine kinase in the PI3K family that regulates protein and lipid production, survival, cell cycle progression, proliferation, and senescence [15, 16]. Sustained and enhanced activation of mTOR signalling can be driven by circulating nutrients, growth factors, and proinflammatory cytokines [17, 18]. Identifying its key role in growth and proliferation (but not limited to), researchers have also showcased that mTOR is deregulated in many diseases (other than inflammation) such as cancer and fibrosis which makes it an extremely targetable and beneficial approach to the treatment of diseases [19, 20]. Currently, several dual mTOR, as well as mTOR/PI3K inhibitors, are under investigation to treat different solid cancers [21], reflecting that repurposing of these inhibitors may be effective against pathologic pro-fibrotic fibroblasts which prolongs fibrosis. On the other hand, mTOR signalling has been reported to be elevated in lung inflammation and fibrosis [22, 23]. However, considering the link between TGF-β (which is central to fibrosis) and mTOR complexes (mTORC1 and mTORC2), a suitable therapeutic approach may contribute to the dual inhibition of mTOR and TGF-β. Vistusertib (AZ-2014) is a dual inhibitor of mTORC1/mTORC2 which was investigated for various solid cancers [24–26]. Conversely, the anti-fibrotic effect of VSB has not been reported. Therefore, we evaluated the scientific and dose rationale for repositioning VSB as a potential therapeutic agent for IPF.

Methodology

In vitro experimentation

Cell lines and cell culture

RAW 264.7 (Mouse macrophages) and BEAS-2B (Human bronchial epithelial cells) cells were purchased from ATCC and were cultured as described earlier [27]. LL29 cells (lung fibroblasts from IPF patient), primary lung fibroblast cells (DHLF-Diseased (IPF) human lung fibroblasts), and HMVEC-L (Human lung microvascular endothelial cells) were purchased from LONZA (MD, USA) and cultured in Ham's F-12 K, FGF™-2 medium and EGM™-2 MV Microvascular Endothelial Cell Growth Medium-2 respectively. All experiments were performed in three biological repeats using three cell types (early passages) and at the confluence of 70–80%.

LPS stimulation

HMVEC-L or BEAS-2B or RAW 264.7 cells were seeded in 6 well plates at 3×10^5 cells/well seeding density and after attaining 70% confluency, cells were serum starved for 6 h. Post-serum starvation, cells were stimulated with LPS (500 ng/mL for RAW 264.7 cells, and 5 µg/mL for BEAS-2B and HMVEC-L cells) and simultaneously cells were treated with either vistusertib (VSB-1.25, 2.5 and 5 µM) or dexamethasone (DEX- 100 ng/mL) followed by incubation for 18 h. After that, cell supernatant was collected for quantifying inflammatory markers by ELISA and subsequently, cells were harvested for RT-qPCR analysis.

TGF-β stimulation

DHLF or LL29 (3.5×10^5 cells/well) cells were counted and seeded in 35 mm dishes and after reaching 70% confluency, cells were subjected to serum starvation overnight. Post-serum starvation cells were stimulated with TGF-β (5 ng/mL) and treated with either vistusertib (VSB- 1.25, 2.5 and 5 µM) or pirfenidone (PIFD- 500 µM) in serum-free media for the next 48 h as described earlier [28] and then cells were subjected to either gene/protein expression analysis.

In vivo experimentation for BMC-induced pulmonary inflammation and fibrosis

Animals and BMC administration

Male, specific pathogen-free grade C57BL/6 mice, weighing 25–30 g, were used for this study. All animal procedures were accepted by the institutional animal ethics committee, CSIR-IICT, Hyderabad (IAEC-IICT-63-2022). Bleomycin (BMC-3 mg/kg) was injected intratracheally to trigger pulmonary inflammation and fibrosis, and saline was similarly administered to the vehicle group and the VSB alone group to replicate the delivery pattern. For the inflammatory model, on the 7th day after disease induction, mice were randomly divided into 6 groups ($n = 8$): (1) vehicle control, (2) BMC control, (3) BMC + DEX (Dexamethasone- 1 mg/kg, i.p.), (4) BMC + VSB (1.5 mg/kg, oral), (5) BMC + VSB (3 mg/kg, oral) and (6) BMC + VSB (6 mg/kg, oral). The doses of BMC and DEX were selected based on previous studies [29, 30]. The doses of VSB were obtained from the conversion of human dose to mice dose calculation formula and based on the literature on mTOR inhibitors such as rapamycin [31]. The mice were treated once every day from the 7th day until the 15th day, and then on day 15, animals were sacrificed followed by a collection of both lobes of the lung for additional evaluations. Some parts of the right lobe were collected in an RNA isoplus-containing tube for RT-qPCR analysis and the rest of the lung tissue was cut into small pieces for different assays and experiments. The left lobe was gently perfused with formalin buffer to improve fixation, and the tissues were subsequently preserved in formalin buffered solution until the paraffin blocks were made. Further, formalin-fixed tissues were embedded in paraffin and used for histopathology and various tissue staining procedures. For the fibrosis model, the mice were divided into 6 groups ($n = 6$) on the 7th day after modelling: (1) vehicle control, (2) BMC control, (3) BMC + PIFD (50 mg/kg, oral), (4) BMC + VSB (3 mg/kg, oral), (5) BMC + VSB (6 mg/kg, oral) and VSB alone (6 mg/kg, oral). Dosing was given once a day starting from the 7th day till the 21st day. On the last day i.e. 22nd day, all animals were sacrificed after measuring lung function parameters and tissues were collected in the same way as described for the inflammatory model.

Lung function measurements by FlexiVent

Before sacrificing animals on the 22nd day, lung function parameters were evaluated by the FlexiVent system as described earlier [32]. Briefly, animals were anaesthetized with sodium pentobarbital (100 mg/kg) and various pulmonary function parameters were measured. Following the tracheostomy, a cannula was placed into the trachea, and various manoeuvres, including Deep Inflation, SnapShot60, QuickPrime30, and pressure-volume loop, were recorded. Inspiratory capacity (IC) was measured by deep inflation perturbation, whereas with SnapShot60 manoeuvre parameters such as total resistance (Rrs), elastance (Ers), and compliance (Crs) were obtained. The parameters such as tissue damping (G) and tissue elastance (H) that describe the mechanical behavior of the lungs were obtained from

QuickPrime3 perturbation and Static compliance (Cst), Parameter A (estimate of inspiratory capacity), Parameter K (curvature of the PV curve), and area (hysteresis of the lungs) were extracted from a Pressure-Volume loop (PV curve).

Histopathology (H&E), AB-PAS staining, and Masson's trichrome staining

For histopathological studies, formalin-fixed tissue sections (5 µm) were subjected separately to hematoxylin/eosin (H&E), Masson's trichrome, and Alcian Blue periodic acid Schiff's (AB-PAS) staining according to manufacturer's protocols. In whole-lung sections, all histopathological analysis and determinations were made by two independently working examiners in a blinded manner. Images were examined and acquired at 4X and 20X in an Olympus iX81 microscope (Olympus Life Science, Germany).

Immunohistochemistry (IHC)

Formalin-fixed tissue sections (5 µm) were mounted on poly-L-Lysine coated slides and subjected to immunohistochemistry using a VECTASTAIN Elite ABC Universal PLUS kit according to the manufacturer's instructions. In short, the tissue sections were deparaffinized, dehydrated, and rehydrated followed by heat-induced antigen retrieval with either 0.01 M citrate buffer or TE buffer. Then sections were probed with respective primary antibodies overnight and subsequently combined with biotinylated secondary antibodies. Colour development was visualized with an ImmPACT DAB EqV reagent after incubation with a VECTASTAIN Elite ABC reagent. Once appropriate intensity / brownish colour was observed, sections were counterstained with hematoxylin and mounted with DPX mountant. Images were acquired under the light microscope at 20X and at least three fields of view for each image were randomly selected.

Inflammatory cells count by flow cytometry

After dissecting the animals on termination day, lung tissues were collected and rinsed with 1X PBS, dissociated with dissociating enzymes then single-cell isolation was performed, as reported earlier with some modifications [33, 34]. In brief, using a scalpel, lung tissues were minced into tiny portions and these pieces were then incubated in 1X collagenase-hyaluronidase mix and DNase-I solution for 0.5–1 h at 37 °C. Later, homogenous organoid/tissue suspension was trypsinized and then quenched with FBS containing DMEM media followed by straining through a 100 µm cell strainer. Subsequently, the cell suspension was centrifuged at 1500 rpm for 3 min and washed with 1X PBS. After counting the single cells, cells were labelled with CD11b, F4/80, IFN-γ, CD4, and CD8 and allowed to incubate on ice with gentle mixing at 15-minute intervals for 45 min. Further, cells were rinsed with FBS containing PBS and subjected to flow cytometry (BD, Biosciences, USA) and analyzed (acquired 8000 events) using BD accuri software.

RNA isolation, cDNA synthesis and RT-qPCR

Total RNA was extracted from cells or tissue homogenates by the guanidinium isothiocyanate acidic phenol-chloroform method using RNA ISO-PLUS with the standard process. Total RNA purity and concentration were determined using Thermo NanoDrop2000/2000 C spectrophotometer and 1 µg of total RNA was converted to cDNA followed by RT-qPCR analysis was performed for quantifying the relative mRNA expression using $2^{-\Delta\Delta Ct}$ method as described previously [35]. Sequences for all primers were optimized and are listed in Table S1.

Western blot analysis

Total protein samples were isolated by lysis of cells or lung tissue homogenates (10% w/v) using RIPA lysis buffer cocktail followed by BCA protein assay was performed for the estimation of protein concentration. An equal amount of protein content (40 µg) was electrophoresed on SDS-PAGE (8–10%) gel for 2 h and thereafter samples were transferred to PVDF membrane (0.45 µm, Millipore, Billerica, MA, US). The membrane was incubated with BSA (5% w/v prepared in TBST wash buffer) for 1 h to avoid nonspecific binding of proteins. After incubation, blots were probed with primary antibodies overnight at 4 °C. Further, blots were washed with TBST wash buffer and exposed to HRP-conjugated secondary antibody (1:10000). The immunoreactive bands were then developed using an ECL reagent and ImageJ software was used for densitometry analysis.

Cytokines measurement by ELISA

The levels of TNF-α, IL-6, and MCP-1were assessed using commercial ELISA kits according to the manufacturer's instructions.

Determination of nitric oxide (NO) content

Total nitric oxide (NO) content was examined using a commercial detection kit based on the Griess method. Briefly, lung tissues were homogenized in cell lysis buffer and lysates were mixed with Griess reagent in equal volume and then incubated for 10 min in the dark, the absorbance was

measured at 540 nm. NO content (μM) was interpolated for each sample from a standard curve.

Statistical analysis

Statistical analysis was performed using student's t-test (unpaired, two-tailed), one-way or two-way ANOVA (Tukey's or Dunnett's multiple comparison test). The statistical analysis was conducted using Graph Pad Prism version 9. Results were depicted as Mean ± SEM. Values of $p < 0.05$ were considered significant.

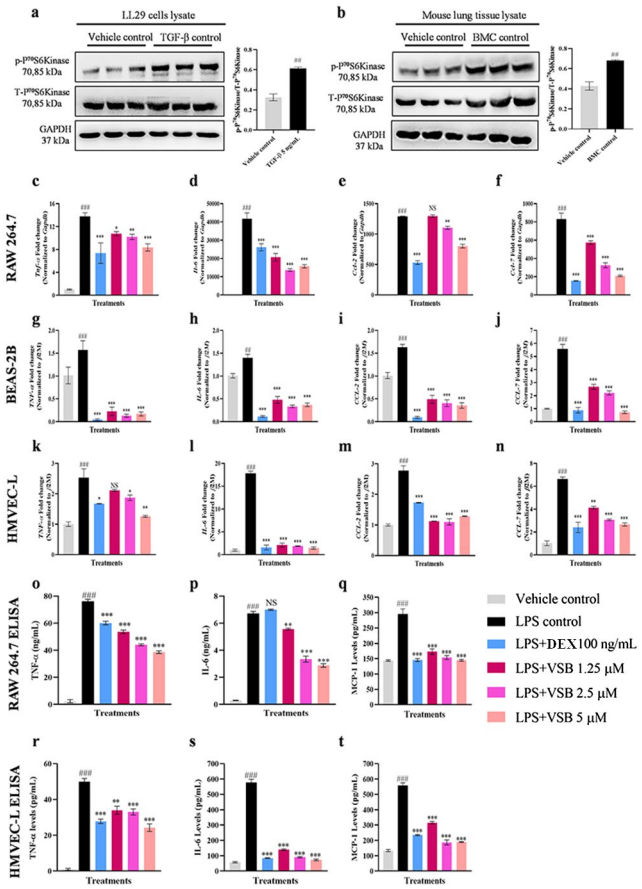

Fig. 1 Vistusertib attenuates inflammatory damage induced by LPS. (**a**) LL29 cells were stimulated with TGF-β and subjected to western blot analysis for specified antibodies. (**b**) In parallel, the C57BL/6 mice were treated intratracheally with vehicle control and bleomycin (3 mg/kg). After 21 days, lung tissues were collected and subjected to immunoblot assay for specified antibodies. (**c-q**) For the inflammatory in vitro model, cells were co-treated with LPS (for RAW 264.7–500 ng/mL and for BEAS-2B and HMVEC-L- 5 μg/mL) and VSB with different concentrations and incubated for 18 h. Expression of pro-inflammatory cytokines were measured by RT-qPCR and ELISA. Gene expression analysis of pro-inflammatory markers in LPS-induced RAW 264.7 (**c-f**), BEAS-2B (**g-j**), and HMVEC-L (**k-n**) cells. ELISA assay was performed using culture media supernatant of LPS-induced RAW 264.7 (**o-q**), and HMVEC-L (**r-t**) cells. Results were depicted as Mean ± SEM ($n = 3$). Values of $^{\#\#}p < 0.01$, and $^{\#\#\#}p < 0.001$ were considered significant between vehicle control vs. LPS control, TGF-β control, or BMC control. Values of $^{*}p < 0.05$, $^{**}p < 0.01$, and $^{***}p < 0.001$ were considered significant between LPS control vs. treatment groups. 'NS' signifies non-significant

Results

Vistusertib inhibits LPS-induced inflammatory markers expression and TGF-β induced fibroblast-differentiation in vitro

The unresolved lung inflammation precedes the development of pulmonary fibrosis as part of a healing process [36–38]. Various inflammatory and fibrotic cascades of genes are known to be modulated by several signalling pathways including mTOR. It was clearly shown that mTOR and its downstream signalling molecules were highly upregulated in IPF patient samples [39]. Similarly, in our study, p-P^{70}S6Kinase and p-mTOR expression levels were highly elevated in both TGF-β stimulated cells and BMC-induced fibrosis tissues (Fig. 1a-b and Fig.S1b-c). In the progression of IPF, inflammation and epithelial cell injury cause further damage to the lungs and a decline in lung functions [40]. Hence, identifying the compounds which have both anti-inflammatory and anti-fibrotic activity could be a viable option to position against IPF. Therefore, we investigated the anti-inflammatory and anti-fibrotic activity of vistusertib on relevant cellular models. To assess the anti-inflammatory activity, the LPS induction model in epithelial cells (BEAS-2B), endothelial cells (HMVEC-L) and macrophages (RAW 264.7) were performed as these cell types play a critical role in disease induction and progression. Further, for anti-fibrotic experiments, the TGF-β induced differentiation model in LL29 and DHLF cells was employed. Before embarking on anti-inflammatory and anti-fibrotic activities, we performed cytotoxicity assays to select safe doses for cell lines. Based on the cell viability assay result (Fig.S2), safe concentrations of VSB (1.25, 2.5, and 5 μM) were selected and validated for further experiments. Next, we assessed the effect of VSB against gene and protein expression of inflammatory markers by RT-qPCR and ELISA respectively in LPS-induced RAW 264.7, BEAS-2B, and HMVEC-L cells. RT-qPCR results showed that gene expression of *Tnf-α, Il-6, Ccl-2*, and *Ccl-7* were significantly ($p < 0.05$) upregulated in LPS-treated cells whereas VSB treatment significantly ($p < 0.05$) downregulated these markers as shown in Fig. 1c-n. Consistent with gene expression changes, the protein levels of inflammatory markers (TNF-α, IL-6, and MCP-1) were significantly ($p < 0.05$) elevated in LPS-induced cells, however, they were reduced when treated with VSB (Fig. 1o-t, Fig. S3) in all three cell types. Similarly, DEX treatment also showed a significant ($p < 0.05$) reduction in

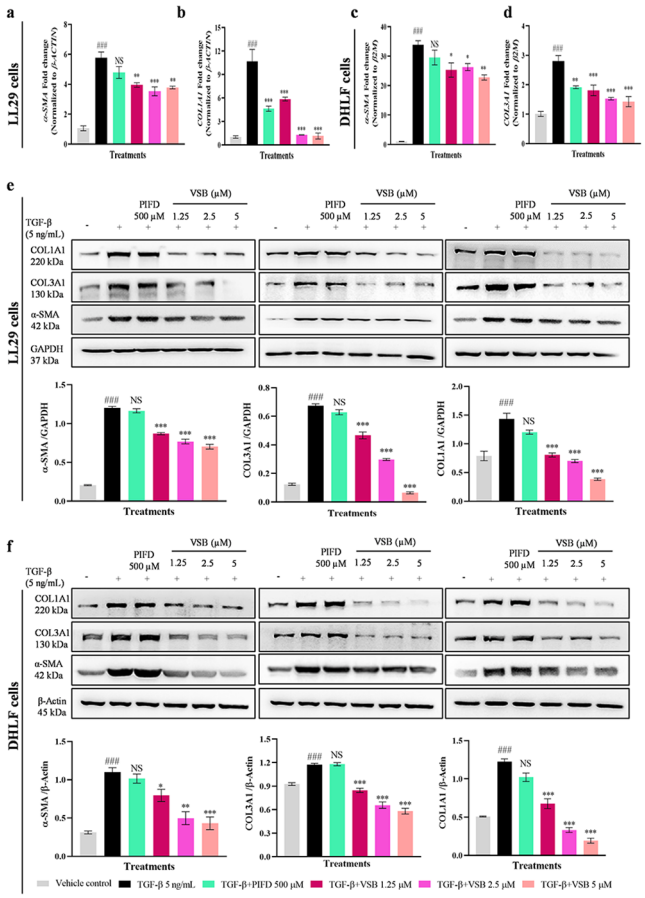

Fig. 2 Vistusertib reduces TGF-β induced fibroblast differentiation and ECM deposition LL29. (**a-b**) or DHLF (**c-d**) cells were co-treated with TGF-β and VSB for 48 h and subjected to RNA isolation, cDNA synthesis followed by RT-qPCR analysis to detect the mRNA levels of *α-SMA* and *COL1A1* or *COL3A1*. In parallel, western blot analysis was performed after co-treatment with TGF-β and VSB or PIFD in LL29 (**e**) or DHLF (**f**) cells. Results were depicted as Mean ± SEM ($n = 3$). Values of $^{###}p < 0.001$ were considered significant between vehicle control vs. TGF-β control. Values of $^{*}p < 0.05$, $^{**}p < 0.01$, and $^{***}p < 0.001$ were considered significant between TGF-β control vs. treatment groups. 'NS' signifies non-significant.

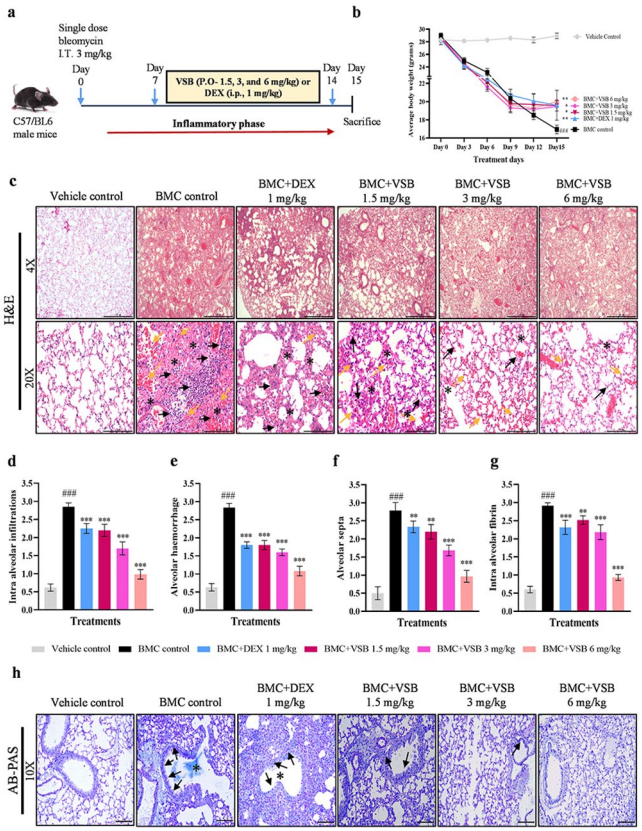

Fig. 3 Treatment with vistusertib alleviates lung injury in bleomycin-induced pulmonary inflammation model. (**a**) The mice were divided into six groups: the vehicle control group, the BMC model group (with bleomycin- 3 mg/kg), BMC + DEX (1 mg/kg) group, BMC + VSB (1.5 mg/kg) group, BMC + VSB (3 mg/kg) group, BMC + VSB (6 mg/kg) group and dosed once daily for 7 days, after 7 days of BMC induction, followed by sacrifice. (**b**) Body weight measurement. (**c-g**) H&E staining and semi-quantitative analysis for intra-alveolar infiltration (black arrow), alveolar hemorrhage (yellow arrow), septum congestion (black asterisk), and intra-alveolar fibrin in mice pulmonary sections. (**h**) Goblet cell hyperplasia (black arrow) and mucin deposition (black asterisk) was assessed by the AB-PAS Staining. Results were depicted as Mean ± SEM ($n = 5$). Values of $^{###}p < 0.001$ were considered significant between vehicle control vs. BMC control. Values of $^{*}p < 0.05$, $^{**}p < 0.01$, and $^{***}p < 0.001$ were considered significant between BMC control vs. treatment groups

levels of these inflammatory markers in LPS-stimulated cells.

Transition of fibroblast to myofibroblast (differentiation) and excessive collagen deposition are crucial events in the development of fibrosis. RT-qPCR and western blot analysis of fibrotic markers in TGF-β induced LL29 cells showed elevated levels of *COL1A1*, *COL3A1* and *α-SMA*, compared to control cells. On the other hand, treatment with VSB significantly ($p < 0.05$) lowered the same (Fig. 2a-b, and e). In line with LL29, DHLF cells also exhibited similar results (Fig. 2c-d, and f). Western blot analysis showed that treatment with pirfenidone did not change protein levels of fibrotic markers in both cell lines (LL29 and DHLF). Taken together, our data suggests that VSB inhibited inflammatory and fibrotic injury in vitro.

Vistusertib attenuates early alveolar inflammation in a murine model of bleomycin-induced pulmonary inflammation

Bleomycin-induced lung injury/fibrosis is a sequential process, upon bleomycin administration AEC injury/death promotes the inflammation and immune cell infiltration for 14 days. Then these events stimulate the fibrotic cytokine expressions and fibroblast proliferation which eventually progress to pulmonary fibrosis [41]. Hence, to check the effect of VSB on inflammation, the bleomycin-induced pulmonary inflammation model was adapted as shown in the schematic representation in Fig. 3a. On the 15th day of

intratracheal bleomycin (BMC) injection, with or without VSB treatment, the mice from the inflammatory model were weighed and euthanized, and lung tissue samples were taken for further investigation. Body weight analysis revealed that body weights in all the groups except sham control were progressively reduced (Fig. 3b). However, compared to BMC control, VSB-treated mice significantly ($p < 0.05$) improved their body weights. Further, as visualized in Fig. 3c-g, hematoxylin and eosin (H&E) staining of lung tissues showed intact alveoli and lung architecture in the vehicle control group, while with BMC induction lung tissues exhibited obvious intra-alveolar infiltration of inflammatory cells, damage to the lung architecture, alveolar haemorrhage accompanying septal thickness, and disturbed array of fibrin in the alveolar cavity. In contrast, DEX or VSB treatment markedly mitigated the alveolar inflammation/infiltration of cells and reduced the overall alveolar damage. Goblet cell hyperplasia, indicative of bronchial remodelling, was examined by AB-PAS staining, and the results revealed a significant increase in the number of goblet cells and mucus deposition in BMC control animals compared to the sham control group. On the other hand, VSB treatment reduced the number of goblet cells and mucin deposition (Fig. 3h).

VSB inhibits the expression of inflammatory markers in the BMC-induced lung inflammation model

To determine the extent of inflammatory reaction under the intervention of VSB in the BMC-induced lung inflammation model, pro-inflammatory markers and macrophage markers were examined. As shown in Fig. 4a-d, the mRNA levels of pro-inflammatory markers such as *Tnf-α*, *Il-1β*, *Ccl2*, and *Ccl7* in the BMC group were significantly ($p < 0.05$) higher compared to the vehicle control group, however, the expression of these cytokines and chemokines were significantly ($p < 0.05$) decreased in the groups which were treated with VSB. Alteration in the phenotype of macrophages and their derived molecules impacts the initiation and pathogenesis of several acute or chronic pulmonary diseases, including acute lung injury (ALI), fibrosis (IPF), allergic asthma, acute respiratory distress syndrome (ARDS), COVID-19, and chronic obstructive pulmonary disorder (COPD) [42]. Therefore, we investigated the expression levels of macrophage and inflammatory markers such as CD68 (Cluster of differentiation-68), F4/80, and MCP-1 (Monocyte chemoattractant protein-1) in mouse lung tissues of the inflammatory model. IHC staining results showed that BMC administration remarkably increased the levels of MCP-1, F4/80, and CD68 in lung tissues compared to the vehicle control group, and treatment with VSB showed a reduction of these markers in a dose-dependent manner (Fig. 4e, S4; Table 1). Furthermore, cell-specific surface markers of immune cells such as $CD11b^{+}F4/80^{+}$ (marker for dendritic cells), IFN-γ^{+}, $CD4^{+}$, and $CD8^{+}$ (markers for T-cells) were analyzed in lung tissues by performing flow cytometry. As

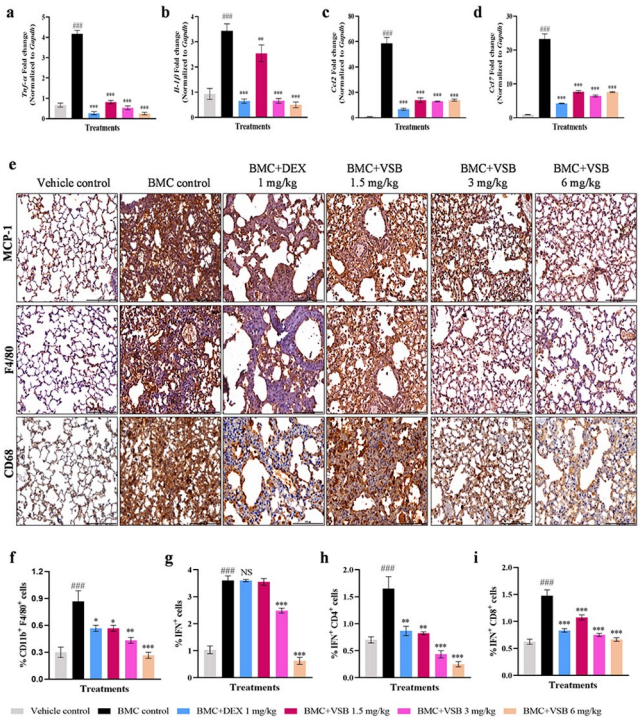

Fig. 4 VSB lessen the inflammatory load by moderating the expression of inflammatory cells/markers in BMC-induced lung inflammation Bleomycin (BMC) intratracheal administration was used for induction of lung injury in mice and after 7 days of BMC instillation mice were treated with or without VSB once daily for 7 days. Upon sacrifice, the lung tissue was excised and were collected for downstream experiments. Lung tissues collected in TRIzol-containing tubes were subjected to RNA isolation, and cDNA synthesis followed by RT-qPCR analysis to detect the mRNA levels of (**a**) *Tnf-α*, (**b**) *Il-1β*, (**c**) *Ccl2*, and (**d**) *Ccl7*. (**e**) Immunohistochemistry (IHC) was performed to detect expression levels of macrophage and inflammatory markers such as CD68, F4/80, and MCP-1. (**f-i**) Part of the lung tissue was isolated and subjected to single-cell isolation followed by flow cytometry analysis for specific inflammatory cell's surface markers. Results were depicted as Mean ± SEM ($n = 5$). Values of $^{\#\#\#}p < 0.001$ was considered significant between vehicle control vs. BMC control. Values of $^{*}p < 0.05$, $^{**}p < 0.01$, and $^{***}p < 0.001$ were considered significant between BMC control vs. treatment groups. 'NS' signifies non-significant

Table 1 Semi-quantitative estimation of inflammatory markers expression in mouse lung tissue sections

Animal Groups	MCP-1 Intensity	F4/80 Intensity	CD68 Intensity
Vehicle control	+	+	++
BMC control	++++	+++	++++
BMC + DEX 1 mg/kg	++	+	+
BMC + VSB 1.5 mg/kg	+++	++	+++
BMC + VSB 3 mg/kg	++	+	+
BMC + VSB 6 mg/kg	+	+	+

indicated in Fig. 4f and Fig. S5a, results revealed that the $CD11b^+$ $F4/80^+$ cell population were meagre in normal lung tissues but significantly ($p < 0.05$) augmented in the BMC group. Treatment with VSB dose-dependently reduced the $CD11b^+F4/80^+$ population. Moreover, there was an increase in the number of IFN-γ^+, IFN-γ^+ $CD4^+$, and IFN-γ^+ $CD8^+$ lymphocytes in the disease control (BMC) group. Interestingly, VSB treatment significantly ($p < 0.05$) moderated the accumulation of macrophages and lymphocytes (T-cells) in BMC-injured lung tissues (Fig. 4g-i and Fig. S5b-d). Altogether these findings revealed that VSB treatment reversed the BMC-induced anomalies by reducing inflammatory cells and their generated molecules, resulting in diminished inflammation.

VSB protects against oxidative stress in the BMC-induced pulmonary inflammation model

Several studies have proven oxidative stress (altered levels of redox system components) as a crucial player in the aetiology of pulmonary fibrosis [7, 43]. To address the effect of VSB on oxidative stress, nitric oxide (NO) production (an indicator of the oxidative process) was determined in animal tissue samples and results revealed that, in response to BMC instillation, the NO generation was significantly ($p < 0.05$) increased in the BMC group, while treatment with DEX or VSB reduced the excessive NO levels (Fig. 5a). Further, we investigated the antioxidant role of VSB in lung tissues using gene expression, and protein expression analysis. RT-qPCR results for *Nrf2* and *Ho-1* (Heme oxygenase-1) mRNA showed that mRNA levels of *Nrf2* and *Ho-1* were downregulated in BMC-treated lung tissues and reversed in DEX or VSB-treated lung tissue samples (Fig. 5b and c). On the other hand, increased gene and protein expression of *Keap-1* was observed in BMC-treated animal samples as compared to vehicle control samples, however, the VSB-treated groups showed reduced *keap-1* expression in a dose-dependent manner (Fig. 5d-f). Further, to check the effect of oxidative stress-induced damage in lung tissues, IHC was performed for myeloperoxidase, neutrophil elastase and mucin5AC. IHC staining demonstrated that control animals had limited MPO, NE, and mucin-5AC expression (indicates reduced immunolabelled positive cells) whereas the BMC-treated group showed elevated levels of these proteins. On the other hand, treatment with BMC + DEX (1 mg/kg) group, BMC + VSB (1.5, 3 or 6 mg/kg) group effectively reduced the staining levels of MPO, NE, and mucin5AC compared to the BMC-treated group (Fig. 5g, S6; Table 2).

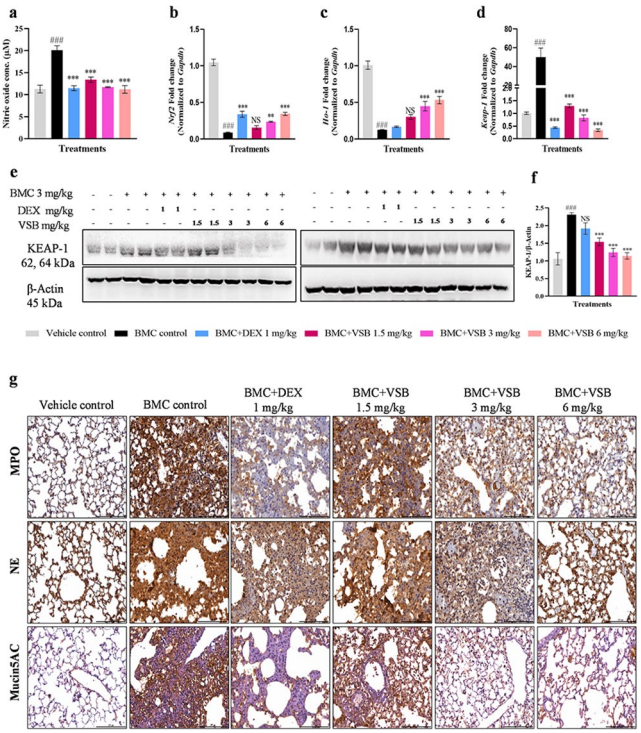

Fig. 5 Administration of VSB improves the oxidative stress in the BMC-induced pulmonary inflammation model. Bleomycin (BMC) intratracheal administration was used for induction of lung injury in mice and after 7 days of BMC instillation mice were treated with or without VSB once daily for 7 days. Upon sacrifice, the lung was excised and lung tissues were collected for downstream experiments. (**a**) Quantification of nitric oxide (NO) levels in lung tissue. (**b-c**) RT-qPCR analysis of *Nrf-2*, and *Ho-1*. (**d-f**) RT-qPCR analysis and western blot analysis for KEAP-1 in lung tissues. (**g**) IHC results for myeloperoxidase (MPO), neutrophil elastase (NE), and Mucin5AC expression levels in lung sections. Results were depicted as Mean ± SEM ($n = 5$). Values of $^{###}p < 0.001$ were considered significant between vehicle control vs. BMC control. Values of $^{**}p < 0.01$, and $^{***}p < 0.001$ were considered significant between BMC control vs. treatment groups. 'NS' signifies non-significant

Table 2 Semi-quantitative estimation of oxidative stress markers expression in mouse lung tissue sections

Animal Groups	MPO Intensity	NE Intensity	Mucin5AC Intensity
Vehicle control	+	+	+
BMC control	+++	+++	++
BMC + DEX 1 mg/kg	++	++	+
BMC + VSB 1.5 mg/kg	+++	+++	++
BMC + VSB 3 mg/kg	++	++	+
BMC + VSB 6 mg/kg	+	+	+

VSB improves the BMC-induced elevation of lung index, and anomalies of pulmonary architecture and reduces the collagen deposition in pulmonary fibrosis tissues

The establishment of the bleomycin-induced pulmonary fibrosis model lasted 3 weeks as shown in Fig. 6a1, and mice's body weights were recorded throughout the experiment. VSB treatment substantially improved body weight (Fig. 6a2) and lung index (Fig. 6b) in comparison to the BMC-challenged group and PIFD-treated group. However, VSB alone treatment did not cause any alterations in the lung index compared to the control group (Fig.S7). To examine the degree of fibrosis and collagen deposition, H&E and Masson's trichrome staining were executed. As presented in Fig. 6c, compared with those of the vehicle control group, the lung tissues in the BMC group showed loss of alveolar architecture, inflammatory cell infiltration, interstitial septal thickening, fibroblast proliferation and collagen deposition, ultimately resulting in severe lung tissue damage. However, VSB attenuated the pathological alterations in the lung tissue. Masson's trichrome staining (Fig. 6d) showed massive deposits of collagen in the interstitial septum of lung tissues in the BMC group, on the other hand, PIFD or VSB treatment reduced the burden of the collagen deposits. BMC group exhibited elevated pathological abnormalities (Ashcroft and fibrotic score), and VSB treatment showed a significant ($p<0.05$) reduction (in a dose-dependent manner) of Ashcroft score compared to BMC control (Fig. 6e-f). On the other hand, VSB treatment alone did not cause any abnormal pathological changes in lung tissues compared to the control (Fig. 6g).

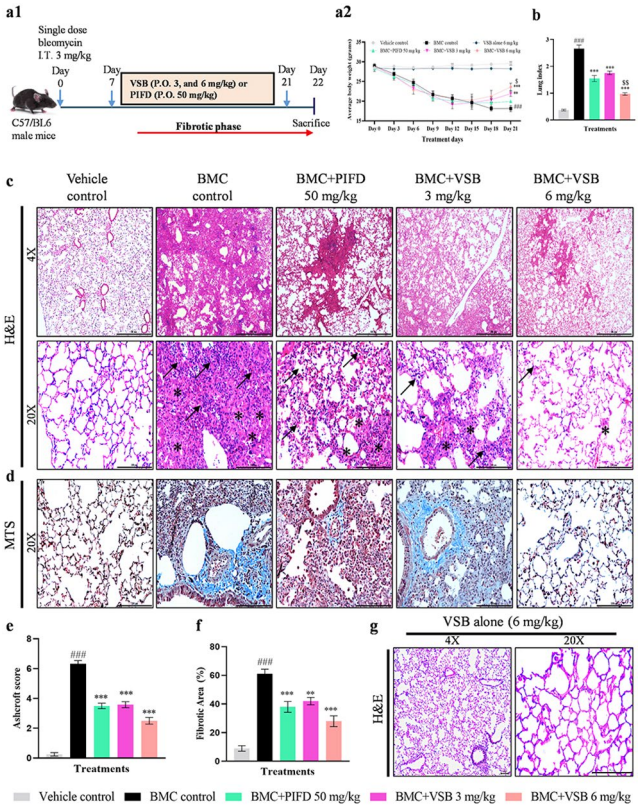

Fig. 6 Treatment with VSB restores morphological and pathological alterations in BMC-induced pulmonary fibrosis tissues. (**a**1) The schematic representation for the establishment of the bleomycin-induced pulmonary fibrosis model which lasted for 3 weeks where mice were treated with or without VSB after 7 days of BMC administration for 14 days (once daily), and during this period, the body weights of mice were recorded (**a**2). Animals were sacrificed on day 22 (after BMC induction) and the lung was excised for performing the downstream experiments. (**b**) Lung index. (**c**) H&E analysis (**d**) collagen deposits (blue) in mice lung sections were assessed by Masson's trichrome staining. (**e-f**) semi-quantitative analysis for Ashcroft score and fibrotic area. (**g**) H&E analysis of VSB alone group animal tissues. Images were visualized in 4X and 20X magnifications under a microscope. Alterations in lung morphology: Inflammatory cell infiltration (black arrow) and collagen deposition (black asterisks). Results were depicted as Mean ± SEM ($n=5$). Values of $^{\#\#\#}p<0.001$ were considered significant between vehicle control vs. BMC control. Values of $^{*}p<0.05$, $^{**}p<0.01$, and $^{***}p<0.001$ were considered significant between BMC control vs. treatment groups. Values of $\$p<0.05$, and $\$\$p<0.01$ were considered significant between the PIFD group vs. VSB treatment groups

Vistusertib treatment improves pulmonary function after BMC challenge

In pulmonary fibrosis, degenerative processes damage not just the alveoli but also other components of the respiratory system, such as the lung vasculature and conducting airways, resulting in a substantial reduction of lung function [44, 45]. In lung fibrosis, certain features are known to increase, such as resistance, elastance, and tissue damping, and concomitantly few parameters, such as inspiratory capacity and compliance, are known to decline [46–48]. Therefore, to investigate the protective effects of VSB in BMC-induced pulmonary fibrosis mice, we measured integrated respiratory mechanics using the FlexiVent system on day 22 after BMC induction. As expected, in the BMC group, a significant ($p<0.05$) reduction in levels of parameters such as inspiratory capacity (IC), compliance (Crs, Cst), total lung capacity (A), and shape constant (K) were observed (Fig. 7a-e and Table S2). At the same time, values of resistance (Rrs), elastance (Ers), tissue damping (G), tissue elastance (H), and area (hysteresis) were significantly ($p<0.05$) upregulated in the BMC-treated group (Fig. 7f-j and Table S3). In contrast, VSB or PIFD treatment showed values similar to those of vehicle control group values, suggesting that VSB treatment effectively restored the BMC-induced impaired mechanical behavior of the lung. Further, we have also measured the lung functional parameters in the VSB alone group, compared to the vehicle control group, VSB treatment did not cause significant changes in

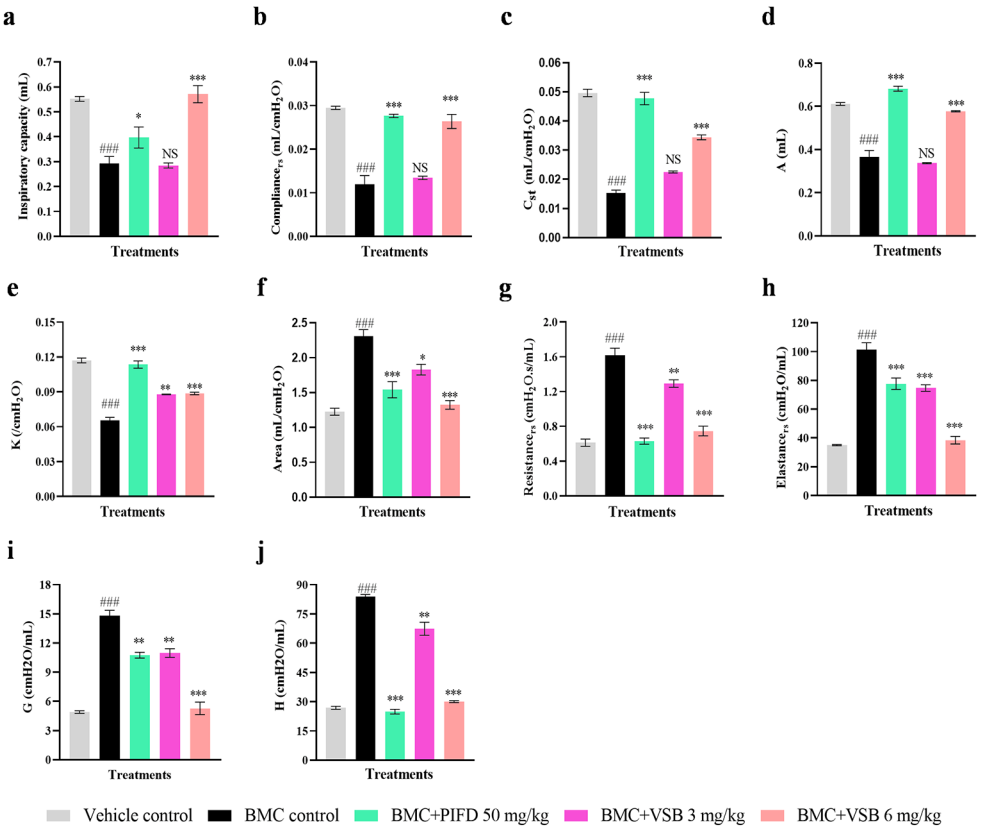

Fig. 7 BMC-induced abnormal pulmonary functional parameters were restored by VSB treatment. (**a-j**) Bleomycin (BMC)-induced pulmonary fibrosis model was used for induction of lung fibrosis in mice and after 7 days of BMC instillation, mice were treated with or without VSB once daily for 14 consecutive days. After the experimental period, mice were subjected to lung functional analysis using a flexiVent system ($n = 5$). Results were depicted as Mean ± SEM. Values of $^{\#\#\#}p < 0.001$ were considered significant between vehicle control vs. BMC control. Values of $^{*}p < 0.05$, $^{**}p < 0.01$, and $^{***}p < 0.001$ were considered significant between BMC control vs. treatment groups. 'NS' signifies non-significant

inspiratory capacity, compliance, respiratory resistance and elastance parameters (Fig. S8).

Vistusertib attenuates BMC-induced pulmonary fibrosis via inhibiting mTOR signalling

Next, to elucidate molecular insights into the anti-fibrotic activity of VSB treatment, we performed RT-qPCR and immunoblot analysis using lung tissues against various fibrotic markers. As presented in Fig. 8a-f, gene expression of *Mmp-9*, *Il-17a*, *Tgf-β*, *α-Sma*, *Col1a1*, and *Col3a1* were significantly ($p < 0.05$) upregulated in the BMC-treated group compared to vehicle control. On the other hand, the treatment with either PIFD or VSB showed downregulation of these fibrotic markers in a dose-dependent manner. Interestingly treatment with VSB alone, slightly reduced the fibrotic markers expression (*Tgf-β*, *α-Sma*, and *Col3a1*), however, they were not significant (Fig. S9). In line with gene expression data, immunoblot results revealed that protein expression of TGF-β, α-SMA, ECM deposition and EMT markers (FN1 and MMP2) were elevated in the BMC-treated group, whereas VSB treatment reversed the BMC-induced expression of these markers dose-dependently (Fig. 8g, Fig. S10), indicating that VSB treatment re-programmed the fibrotic cascade in lung tissues. Pirfenidone is known to inhibit the TGF-β signaling and its downstream signaling markers expression such as α-SMA, MMP2, FN1 and collagen [49, 50]. In our study as well, PIFD treatment also significantly reduced the BMC-induced fibrotic marker expression however E-cad levels were not altered compared to BMC. Emerging evidence confirmed a critical role of mTOR signalling in the pathogenesis of IPF by its involvement in ECM production, fibroblast proliferation, survival, and metabolism [51, 52]. Therefore, to check whether mTOR signalling gets activated upon bleomycin induction, we evaluated protein levels of mTOR and its well-known downstream effector i.e., P^{70}S6Kinase using immunoblot assay. Results of western blot (Fig. 8h, Fig. S4) showed a marked increase in p-mTOR and p-P^{70}S6Kinase levels in the BMC-treated group as compared to the vehicle control group and further VSB treatment reduced the ratio of p-mTOR/total mTOR and p- P^{70}S6Kinase/total P^{70}S6Kinase, indicating anti-fibrotic activity of VSB might be via this pathway.

Discussion

Idiopathic pulmonary fibrosis (IPF) is a form of interstitial lung disease in which excessive fibroblast proliferation and extracellular matrix promote remodelling of the lung architecture, leading to respiratory insufficiency. Several

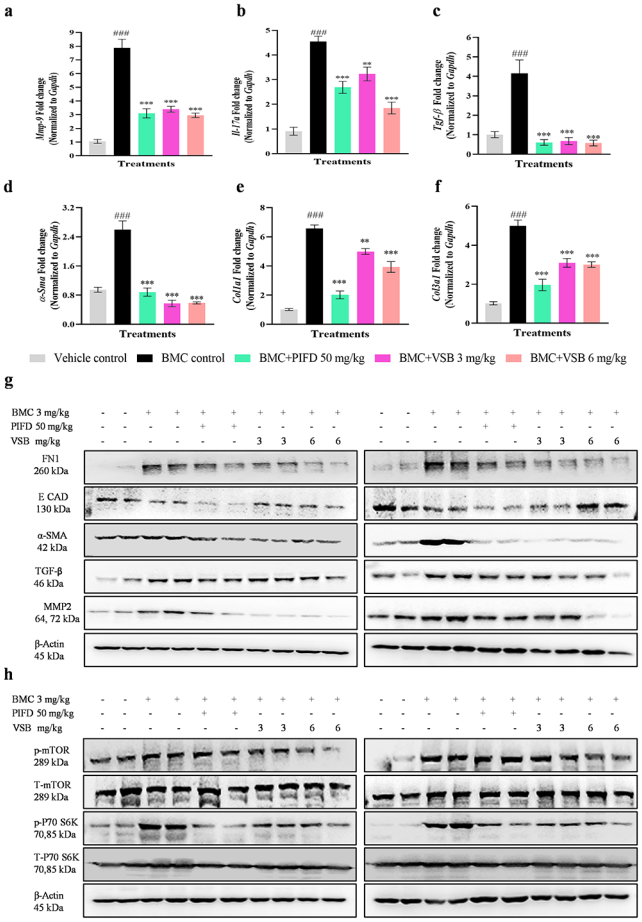

Fig. 8 Vistusertib attenuates BMC-induced pulmonary fibrotic markers by inhibiting mTOR signaling. After sacrificing the animals, lung tissues were collected, snap-frozen and then lung tissues processed for downstream experiments. (**a-f**) Lung tissues collected in RNA isoplus-containing tubes were subjected to RNA isolation, and cDNA synthesis followed by RT-qPCR analysis to detect the specified mRNA levels. (**g**) Lung tissues were homogenized and lysed with RIPA lysis buffer cocktail for protein isolation. The protein expressions in lung tissues were analyzed by immunoblot assay using the specified fibrotic antibodies. (**h**) Western blot analysis for specified mTOR pathway components. Results were depicted as Mean ± SEM ($n = 4$). Values of $^{###}p < 0.001$ were considered significant between vehicle control vs. BMC control. Values of $^{**}p < 0.01$, and $^{***}p < 0.001$ were considered significant between BMC control vs. treatment groups

pathways namely, TGF-β/SMAD, Wnt/β-catenin and mTOR play a key role onset and maintenance of IPF. Due to the poor understanding of pathophysiology, low survival rate and limited therapeutic efficacy of FDA-approved medications, repurposing of marketed drugs is desirable for better treatment outcomes [53, 54]. Several studies reported that mTOR signalling was significantly elevated in lung inflammation and IPF patient lung samples compared to the control. Investigating the compounds which modulate derailed pathways would pave a path for translational outcomes. Vistusertib is a dual inhibitor of mTORC1/mTORC2 and has been under clinical investigation for various diseases including cancer [55–57]. Therefore, in the present study, we investigated potential anti-inflammatory and anti-fibrotic activities of vistusertib (VSB) against in vitro and in vivo models. Our results demonstrated that VSB showed promising anti-inflammatory and anti-fibrotic effects against LPS-induced inflammation and TGF-β induced differentiation in vitro models. Our results further explored the protective role of VSB on BMC-induced lung inflammation and fibrosis murine model. Following BMC instillation, VSB therapy effectively reduced lung damage and fibrosis by lowering inflammatory burden and oxidative stress, which resulted in decreased fibrotic marker expression and better lung function.

Several research studies indicated that incidents of foreign entities with cytopathic effects led to early pulmonary epithelial and endothelial injury that calls for various inflammatory and immune effector cells by releasing a network of inflammatory mediators, cytokines, chemokines, and growth factors resulting in the aid of alveolar damage. Further, the impairment in this healing process contributes to the non-reversible fibrosis [58, 59]. Upon activation by inflammatory stimuli (either bacterial or viral infections), macrophages and monocytes are stimulated and secrets the major cytokines (such as TNF-α, interleukins, and chemokines (CCL2, CCL8, and CCL7) to fight against the pathogens [60–63]. Bleomycin is an antibiotic with potent anti-cancer activity but has limited use due to its pulmonary toxicity. Bleomycin-induced lung injury initiates cytokine, chemokine releases and induces oxidative stress which further triggers the inflammation, and then ultimately leads to fibroblast differentiation into myofibroblasts causing extracellular matrix deposition, and the development of fibrosis at days 10–21. Considering this, the intratracheal (IT) administration of bleomycin to rodents is commonly accepted as an in vivo model to investigate both inflammatory and fibrotic alterations in the lung interstitium [64, 65]. Similarly, in the present study, for investigating the anti-inflammatory response of VSB, we employed LPS treatment in vitro (all three cell types i.e., BEAS-2B, HMVEC-L, and RAW 264.7 that are involved in the rescue from lung injury) and early stage of BMC-induced pulmonary fibrosis model i.e., lung inflammation in in vivo. Consistently our results indicated that in LPS or BMC treatment (inflammation model), gene and protein expression levels of inflammatory mediators such as TNF-α, IL-1β, IL-6, CCL2, and CCL7 were significantly elevated accounting for the presence of extensive inflammatory infiltrate. It is reported that in ILD mice models, MCP-1 stimulates collagen formation and deletion of the CCR2 (receptor for MCP-1) protects against lung fibrosis [66]. Methyl-CpG-binding domain protein 2 (MBD2) was found to be altered in macrophages in BMC-induced lung fibrosis and IPF patients. Deletion of MBD2

reduced lung fibrosis by mitigating the TGF-β1 production and $CD206^{+}CD68^{+}F4/80^{+}$ macrophage accumulation, indicating that, $CD68^{+}F4/80^{+}$ plays a critical role in ameliorating fibrosis [67]. Our IHC (for MCP-1, CD68 and F4/80) and flow cytometry data from the inflammatory model also showed an accumulation of macrophages and other inflammatory cellular infiltrates (supporting pulmonary histological changes) upon induction with BMC. However, VSB treatment showed a marked reduction of inflammatory cells and their derived molecules favoring the alleviation of inflammatory response. Dexamethasone is a potent glucocorticoid that inhibits neutrophil migration, lymphocyte proliferation and regulates proinflammatory cytokines such TNF-α, interleukins, and chemokines [68, 69]. DEX demonstrated its anti-inflammatory properties in the current investigation by impeding the cytokine response and reducing the inflammatory and immune cell accumulation in lung tissues.

Accumulating evidence suggested that oxidative stress resulting from the dysregulated release of neutrophil extracellular trap components such as neutrophil elastase (NE), myeloperoxidase (MPO), histones, and DNA contributes significantly to the pathogenesis of lung diseases such as cystic fibrosis, COPD, acute lung injury, acute respiratory distress syndrome and pulmonary fibrosis [70, 71]. Moreover, some of the factors such as neutrophil elastase, oxidative stress, and NO (nitric oxide) induce the expression of mucin5AC (a biomarker of IPF) in respiratory epithelial cells [72–74]. It was known that mTOR plays a crucial role in regulating oxidative stress by increasing mitochondrial biogenesis and oxidative metabolism via modulating the PGC-1α pathway [75]. It was shown that mTOR controls the dysfunction of endothelium induced by oxidative stress, and the blocking of mTORC1 restores eNOS function, enhances NO synthesis, and prevents O_2-formation in the aorta of rats [76]. It has been demonstrated that IPF patients have elevated levels of 8-isoprostane, an oxidative stress biomarker [77], exhaled NO, and iNOS expression in their lung tissues [78]. These results imply that oxidative and nitrosative stress are more prevalent in IPF patients. Therefore, targeting oxidative stress as anti-fibrotic therapy in IPF may improve some aspects of the disease. In our study, in vivo results suggested that greater oxidative stress load was developed after BMC instillation which can be seen by elevated levels of NE, MPO, mucin5AC, NO, and Keap1 and reduced levels of Nrf2 along with HO-1 in BMC-treated lung tissues. Notably, a reversal of these results was observed in the VSB treatment group demonstrating the potential anti-oxidant role of VSB via induction of Nrf2/HO-1. Nrf2 mediates the up-regulation of several antioxidant enzymes and is known to inhibit lipid peroxidation, indicating that Nrf2 plays a protective role in the resolution of fibrosis by elevating the Nrf2 target gene expressions [79]. In supporting these mechanisms, elevated levels of MPO [80], NE [81], and mucin5AC [82] in $Nrf2^{-/-}$ mice were observed in various lung disease models. It was also reported that reduction of MPO and NE levels with augmentation of NRF2 and HO-1 levels reduced the severity of the LPS-induced lung inflammation in rat models [83].

Furthermore, similar to previous findings [84], our results showed elevated levels of myofibroblast marker (α-SMA), ECM production and deposition markers (presence of collagen fibers or collagen protein, MMP2, MMP9) expression in TGF-β induced differentiation models and BMC-induced lung fibrotic tissues. Additionally, the expression of EMT markers (E-CAD and FN1) were altered in BMC-induced fibrosis samples. Since TGF-β1 is thought to be a powerful fibrosis driver and is elevated in patients with fibrotic disorders such as renal, pulmonary, and hepatic fibrosis, this enhanced expression of overall fibrotic markers may be the result of elevated TGF-β1 levels [85]. These cellular and molecular amendments make gaseous exchange more difficult for the lungs to carry out and ultimately lead to a decline in lung function [47]. Our findings showed that VSB treatment ameliorated fibrosis and improved lung function. However, TGF-β-induced fibrosis was further provoked by activated mTOR signalling and VSB treatment suppressed mTOR pathway activation. These results indicate that inhibiting the mTOR pathway might be effective for fibrosis resolution.

In summary, VSB treatment inhibited inflammatory response by lowering the accumulation of cellular inflammatory infiltrate and expression of pro-inflammatory cytokines (TNF-α), interleukins (IL-1β, IL-6), and chemokines (CCL2, CCL7) in vitro and in vivo model of lung injury, and protected against oxidative stress by reducing oxidative stress markers such as MPO, NE, mucin5AC and NO content via modulating Nrf2/HO-1/keap1 signalling pathway. On the other hand, the anti-fibrotic activity of VSB resolved fibrosis by improving lung function, histopathology, and fibrotic marker expression through suppressing mTOR signalling.

Conclusion

Overall, our data showed that the anti-inflammatory, anti-oxidative, and anti-fibrotic activities of VSB could be considered an attractive and effective treatment option for therapeutic usage against pulmonary fibrosis.

Supplementary Information The online version contains supplementary material available at https://doi.org/10.1007/s00011-024-01894-5.

Acknowledgements Authors thank the Director, CSIR-IICT, Hyderabad, India, for providing the facilities and funding necessary for the conducting of this work. T.B.S acknowledges the Council of Scientific and Industrial Research, New Delhi for providing SRF. Authors acknowledges Dr Ramesh Ummanni for help on mTOR antibodies.

Author contributions Conceptualization: S.R.K, S.B.A; Methodology: T. B.S, S.B.A; In vitro cell culture: T.B.S.; RT-qPCR, Western-blot analysis: T.B.S; In vivo experiments: T.B.S, S.B.A, and C.Yogesh; Manuscript writing - review & editing: T.B.S, S.B.A, and S. R. K.; funding acquisition: S.R.K and S.B.A.

Funding Used internal funds of the institute. This research did not receive any specific grant from funding agencies in the public, commercial, or not-for-profit sectors.

Data availability No datasets were generated or analysed during the current study.

Declarations

Competing interests The authors declare no competing interests.

References

1. Raghu G, Remy-Jardin M, Richeldi L, Thomson CC, Inoue Y, Johkoh T, et al. Idiopathic pulmonary fibrosis (an update) and progressive pulmonary fibrosis in adults: an Official ATS/ERS/JRS/ALAT Clinical Practice Guideline. Am J Respir Crit Care Med. 2022;205:e18–47. https://doi.org/10.1164/rccm.202202-0399ST.
2. Alsomali H, Palmer E, Aujayeb A, Funston W. Early diagnosis and treatment of idiopathic pulmonary fibrosis: a narrative review. Pulmonary Therapy. 2023;9:177–93. https://doi.org/10.1007/s41030-023-00216-0.
3. Maher TM, Bendstrup E, Dron L, Langley J, Smith G, Khalid JM, et al. Global incidence and prevalence of idiopathic pulmonary fibrosis. Respir Res. 2021;22:197. https://doi.org/10.1186/s12931-021-01791-z.
4. Phan THG, Paliogiannis P, Nasrallah GK, Giordo R, Eid AH, Fois AG, et al. Emerging cellular and molecular determinants of idiopathic pulmonary fibrosis. Cell Mol Life Sci. 2021;78:2031–57. https://doi.org/10.1007/s00018-020-03693-7.
5. Shenderov K, Collins SL, Powell JD, Horton MR. Immune dysregulation as a driver of idiopathic pulmonary fibrosis. J Clin Investig. 2021;131. https://doi.org/10.1172/jci143226.
6. Tran S, Ksajikian A, Overbey J, Li P, Li Y. Pathophysiology of pulmonary fibrosis in the context of COVID-19 and implications for treatment: a narrative review. Cells. 2022;11. https://doi.org/10.3390/cells11162489.
7. Kinnula VL, Fattman CL, Tan RJ, Oury TD. Oxidative stress in pulmonary fibrosis: a possible role for redox modulatory therapy. Am J Respir Crit Care Med. 2005;172:417–22. https://doi.org/10.1164/rccm.200501-017PP.
8. Kuwano K, Hagimoto N, Maeyama T, Fujita M, Yoshimi M, Inoshima I, et al. Mitochondria-mediated apoptosis of lung epithelial cells in idiopathic interstitial pneumonias. Lab Invest. 2002;82:1695–706. https://doi.org/10.1097/01.lab.0000045084.81853.76.
9. Cantin AM, North SL, Fells GA, Hubbard RC, Crystal RG. Oxidant-mediated epithelial cell injury in idiopathic pulmonary fibrosis. J Clin Investig. 1987;79:1665–73. https://doi.org/10.1172/jci113005.
10. Zemans RL, Henson PM, Henson JE, Janssen WJ. Conceptual approaches to lung injury and repair. Annals Am Thorac Soc. 2015;12(Suppl 1):S9–15. https://doi.org/10.1513/AnnalsATS.201408-402MG.
11. Malaviya R, Kipen HM, Businaro R, Laskin JD, Laskin DL. Pulmonary toxicants and fibrosis: innate and adaptive immune mechanisms. Toxicol Appl Pharmcol. 2020;409:115272. https://doi.org/10.1016/j.taap.2020.115272.
12. Heukels P, Moor CC, von der Thüsen JH, Wijsenbeek MS, Kool M. Inflammation and immunity in IPF pathogenesis and treatment. Respir Med. 2019;147:79–91. https://doi.org/10.1016/j.rmed.2018.12.015.
13. Hill C, Jones MG, Davies DE, Wang Y. Epithelial-mesenchymal transition contributes to pulmonary fibrosis via aberrant epithelial/fibroblastic cross-talk. J lung Health Dis. 2019;3:31–5.
14. Ye Z, Hu Y. TGF–β1: gentlemanly orchestrator in idiopathic pulmonary fibrosis (review). Int J Mol Med. 2021;48:132. https://doi.org/10.3892/ijmm.2021.4965.
15. Rahimi RA, Andrianifahanana M, Wilkes MC, Edens M, Kottom TJ, Blenis J, et al. Distinct roles for mammalian target of rapamycin complexes in the fibroblast response to transforming growth factor-beta. Cancer Res. 2009;69:84–93. https://doi.org/10.1158/0008-5472.Can-08-2146.
16. Saxton RA, Sabatini DM. mTOR Signaling in Growth, Metabolism, and Disease. Cell. 2017;168:960–76. https://doi.org/10.1016/j.cell.2017.02.004.
17. Buerger C. Epidermal mTORC1 signaling contributes to the pathogenesis of Psoriasis and could serve as a therapeutic target. Front Immunol. 2018;9:2786. https://doi.org/10.3389/fimmu.2018.02786.
18. Marques-Ramos A, Cervantes R. Expression of mTOR in normal and pathological conditions. Mol Cancer. 2023;22:112. https://doi.org/10.1186/s12943-023-01820-z.
19. Das A, Reis F, Maejima Y, Cai Z, Ren J. mTOR Signaling in Cardiometabolic Disease, Cancer, and aging. Oxidative Med Cell Longev. 2017;2017:6018675. https://doi.org/10.1155/2017/6018675.
20. Lawrence J, Nho R. The role of the mammalian target of Rapamycin (mTOR) in Pulmonary Fibrosis. Int J Mol Sci. 2018;19. https://doi.org/10.3390/ijms19030778.
21. Wu X, Xu Y, Liang Q, Yang X, Huang J, Wang J, et al. Recent advances in dual PI3K/mTOR inhibitors for Tumour Treatment. Front Pharmacol. 2022;13:875372. https://doi.org/10.3389/fphar.2022.875372.
22. Li R, Zou X, Huang H, Yu Y, Zhang H, Liu P et al. HMGB1/PI3K/Akt/mTOR signaling participates in the pathological process of Acute Lung Injury by regulating the maturation and function of dendritic cells. 2020; 11. https://doi.org/10.3389/fimmu.2020.01104.
23. Woodcock HV, Eley JD, Guillotin D, Platé M, Nanthakumar CB, Martufi M, et al. The mTORC1/4E-BP1 axis represents a critical signaling node during fibrogenesis. Nat Commun. 2019;10:6. https://doi.org/10.1038/s41467-018-07858-8.
24. Li Y, Cui JT. Inhibition of Bcl-2 potentiates AZD-2014-induced anti-head and neck squamous cell carcinoma cell activity. Biochem Biophys Res Commun. 2016;477:607–13. https://doi.org/10.1016/j.bbrc.2016.06.100.
25. Huo HZ, Zhou ZY, Wang B, Qin J, Liu WY, Gu Y. Dramatic suppression of colorectal cancer cell growth by the dual mTORC1 and mTORC2 inhibitor AZD-2014. Biochem Biophys Res Commun. 2014;443:406–12. https://doi.org/10.1016/j.bbrc.2013.11.099.
26. Zheng B, Mao JH, Qian L, Zhu H, Gu DH, Pan XD, et al. Preclinical evaluation of AZD-2014, a novel mTORC1/2 dual inhibitor, against renal cell carcinoma. Cancer Lett. 2015;357:468–75. https://doi.org/10.1016/j.canlet.2014.11.012.
27. Tirunavalli SK, Gourishetti K, Kotipalli RSS, Kuncha M, Kathirvel M, Kaur R, et al. Dehydrozingerone ameliorates

Lipopolysaccharide induced acute respiratory distress syndrome by inhibiting cytokine storm, oxidative stress via modulating the MAPK/NF-κB pathway. Phytomedicine: Int J Phytotherapy Phytopharmacology. 2021;92:153729. https://doi.org/10.1016/j.phymed.2021.153729.
28. Shaikh TB, Kuncha M, Andugulapati SB, Sistla R. Dehydrozingerone alleviates pulmonary fibrosis via inhibition of inflammation and epithelial-mesenchymal transition by regulating the Wnt/β-catenin pathway. Eur J Pharmacol. 2023;953:175820. https://doi.org/10.1016/j.ejphar.2023.175820.
29. Liu MH, Lin AH, Ko HK, Perng DW, Lee TS, Kou YR. Prevention of Bleomycin-Induced Pulmonary inflammation and fibrosis in mice by Paeonol. Front Physiol. 2017;8:193. https://doi.org/10.3389/fphys.2017.00193.
30. Cross J, Stenton GR, Harwig C, Szabo C, Genovese T, Di Paola R, et al. AQX-1125, small molecule SHIP1 activator inhibits bleomycin-induced pulmonary fibrosis. Br J Pharmacol. 2017;174:3045–57. https://doi.org/10.1111/bph.13934.
31. Madala SK, Maxfield MD, Davidson CR, Schmidt SM, Garry D, Ikegami M, et al. Rapamycin regulates Bleomycin-Induced Lung damage in SP-C-Deficient mice. Pulmonary Med. 2011;2011:653524. https://doi.org/10.1155/2011/653524.
32. Tirunavalli SK, Kuncha M, Sistla R, Andugulapati SB. Targeting TGF-β/periostin signaling by sesamol ameliorates pulmonary fibrosis and improves lung function and survival. J Nutr Biochem. 2023;116:109294. https://doi.org/10.1016/j.jnutbio.2023.109294.
33. Nakatsuka Y, Yaku A, Handa T, Vandenbon A, Hikichi Y, Motomura Y et al. Profibrotic function of pulmonary group 2 innate lymphoid cells is controlled by regnase-1. Eur Respir J. 2021; 57:2000018. https://doi.org/10.1183/13993003.00018-2020.
34. Tirunavalli SK, Pramatha S, Eedara AC, Walvekar KP, Immanuel C, Potdar P, et al. Protective effect of β-glucan on poly(I:C)-induced acute lung injury/inflammation: therapeutic implications of viral infections in the respiratory system. Life Sci. 2023;330:122027. https://doi.org/10.1016/j.lfs.2023.122027.
35. Andugulapati SB, Gourishetti K, Tirunavalli SK, Shaikh TB, Sistla R. Biochanin-A ameliorates pulmonary fibrosis by suppressing the TGF-β mediated EMT, myofibroblasts differentiation and collagen deposition in in vitro and in vivo systems. Phytomedicine: Int J Phytotherapy Phytopharmacology. 2020;78:153298. https://doi.org/10.1016/j.phymed.2020.153298.
36. Bian F, Lan Y-W, Zhao S, Deng Z, Shukla S, Acharya A, et al. Lung endothelial cells regulate pulmonary fibrosis through FOXF1/R-Ras signaling. Nat Commun. 2023;14:2560. https://doi.org/10.1038/s41467-023-38177-2.
37. Zhao W, Wang L, Wang Y, Yuan H, Zhao M, Lian H et al. Injured endothelial cell: a risk factor for pulmonary fibrosis. 2023; 24:8749.
38. Savin IA, Zenkova MA, Sen'kova AV. Pulmonary Fibrosis as a Result of Acute Lung Inflammation: Molecular Mechanisms, Relevant In Vivo Models, Prognostic and Therapeutic Approaches. 2022; 23:14959.
39. Park JS, Park HJ, Park YS, Lee S-M, Yim J-J, Yoo C-G, et al. Clinical significance of mTOR, ZEB1, ROCK1 expression in lung tissues of pulmonary fibrosis patients. BMC Pulm Med. 2014;14:168. https://doi.org/10.1186/1471-2466-14-168.
40. Knudsen L, Ruppert C, Ochs M. Tissue remodelling in pulmonary fibrosis. Cell Tissue Res. 2017;367:607–26. https://doi.org/10.1007/s00441-016-2543-2.
41. Ishida Y, Kuninaka Y, Mukaida N, Kondo T. Immune mechanisms of Pulmonary Fibrosis with Bleomycin. Int J Mol Sci. 2023;24. https://doi.org/10.3390/ijms24043149.
42. Lee J-W, Chun W, Lee HJ, Min J-H, Kim S-M, Seo J-Y et al. The role of macrophages in the development of Acute and Chronic Inflammatory Lung diseases. 2021; 10:897.
43. Estornut C, Milara J, Bayarri MA, Belhadj N, Cortijo J. Targeting oxidative stress as a Therapeutic Approach for Idiopathic Pulmonary Fibrosis. 2022; 12. https://doi.org/10.3389/fphar.2021.794997.
44. Agustí AG, Roca J, Gea J, Wagner PD, Xaubet A. Rodriguez-Roisin RJARoRD. Mechanisms of gas-exchange impairment in idiopathic pulmonary fibrosis. 2012.
45. Pardo A, Selman M. Idiopathic pulmonary fibrosis: new insights in its pathogenesis. Int J Biochem Cell Biol. 2002;34:1534–8. https://doi.org/10.1016/S1357-2725(02)00091-2.
46. Nava S, Rubini F. Lung and chest wall mechanics in ventilated patients with end stage idiopathic pulmonary fibrosis. Thorax. 1999;54:390–5. https://doi.org/10.1136/thx.54.5.390.
47. Plantier L, Cazes A, Dinh-Xuan A-T, Bancal C, Marchand-Adam S, Crestani B. Physiology of the lung in idiopathic pulmonary fibrosis. Eur Respir Rev. 2018; 27:170062. https://doi.org/10.1183/16000617.0062-2017.
48. Bachofen H, Scherrer M. Lung tissue resistance in diffuse interstitial pulmonary fibrosis. J Clin Investig. 1967;46:133–40. https://doi.org/10.1172/jci105506.
49. Molina-Molina M, Machahua-Huamani C, Vicens-Zygmunt V, Llatjós R, Escobar I, Sala-Llinas E, et al. Anti-fibrotic effects of pirfenidone and rapamycin in primary IPF fibroblasts and human alveolar epithelial cells. BMC Pulm Med. 2018;18:63. https://doi.org/10.1186/s12890-018-0626-4.
50. Roach KM, Castells E, Dixon K, Mason S, Elliott G, Marshall H, et al. Evaluation of Pirfenidone and Nintedanib in a human lung model of Fibrogenesis. Front Pharmacol. 2021;12:679388. https://doi.org/10.3389/fphar.2021.679388.
51. Platé M, Guillotin D, Chambers RC. The promise of mTOR as a therapeutic target pathway in idiopathic pulmonary fibrosis. Eur Respir Rev. 2020; 29:200269. https://doi.org/10.1183/16000617.0269-2020.
52. Peng J, Xiao X, Li S, Lyu X, Gong H, Tan S, et al. Aspirin alleviates pulmonary fibrosis through PI3K/AKT/mTOR-mediated autophagy pathway. Exp Gerontol. 2023;172:112085. https://doi.org/10.1016/j.exger.2023.112085.
53. Mei Q, Liu Z, Zuo H, Yang Z, Qu J. Idiopathic pulmonary fibrosis: an update on Pathogenesis. Front Pharmacol. 2021;12:797292. https://doi.org/10.3389/fphar.2021.797292.
54. Fraser E, Hoyles RK. Therapeutic advances in idiopathic pulmonary fibrosis. Clin Med. 2016;16:42–51. https://doi.org/10.7861/clinmedicine.16-1-42.
55. Plotkin SR, Kumthekar P, Wen PY, Barker FG, Stemmer-Rachamimov A, Beauchamp RL et al. Multi-center, single arm phase II study of the dual mTORC1/mTORC2 inhibitor vistusertib for patients with recurrent or progressive grade II-III meningiomas. 2021; 39:2024–2024. https://doi.org/10.1200/JCO.2021.39.15_suppl.2024.
56. Heudel P, Frenel J-S, Dalban C, Bazan F, Joly F, Arnaud A et al. Safety and Efficacy of the mTOR Inhibitor, Vistusertib, Combined With Anastrozole in Patients With Hormone Receptor−Positive Recurrent or Metastatic Endometrial Cancer: The VICTORIA Multicenter, Open-label, Phase 1/2 Randomized Clinical Trial. JAMA Oncology. 2022; 8:1001–1009. https://doi.org/10.1001/jamaoncol.2022.1047.
57. Jordan JT, Orr CC, Thalheimer RD, Cambillo JV, Beauchamp RL, Shaikh G, et al. Prospective phase II trial of the dual mTORC1/2 inhibitor vistusertib for progressive or symptomatic meningiomas in persons with neurofibromatosis 2. Neuro-oncology Adv. 2023;5:vdad041. https://doi.org/10.1093/noajnl/vdad041.
58. Wynn TA, Ramalingam TR. Mechanisms of fibrosis: therapeutic translation for fibrotic disease. Nat Med. 2012;18:1028–40. https://doi.org/10.1038/nm.2807.
59. Wynn T. Cellular and molecular mechanisms of fibrosis. 2008; 214:199–210. https://doi.org/10.1002/path.2277.

60. Dauphinee SM, Karsan A. Lipopolysaccharide signaling in endothelial cells. Lab Invest. 2006;86:9–22. https://doi.org/10.1038/labinvest.3700366.
61. Meng L, Li L, Lu S, Li K, Su Z, Wang Y, et al. The protective effect of dexmedetomidine on LPS-induced acute lung injury through the HMGB1-mediated TLR4/NF-κB and PI3K/Akt/mTOR pathways. Mol Immunol. 2018;94:7–17. https://doi.org/10.1016/j.molimm.2017.12.008.
62. Hossen I, Kaiqi Z, Hua W, Junsong X, Mingquan H, Yanping C. Epigallocatechin gallate (EGCG) inhibits lipopolysaccharide-induced inflammation in RAW 264.7 macrophage cells via modulating nuclear factor kappa-light-chain enhancer of activated B cells (NF-κB) signaling pathway. 2023; 11:4634–50. https://doi.org/10.1002/fsn3.3427.
63. Arango Duque G, Descoteaux A, Macrophage, Cytokines. Involvement in Immunity and Infectious Diseases. 2014; 5. https://doi.org/10.3389/fimmu.2014.00491.
64. Reinert T, Baldotto CSR, Nunes FAP, Scheliga AAS. Bleomycin-Induced Lung Injury. J Cancer Res. 2013;2013:480608. https://doi.org/10.1155/2013/480608.
65. Izbicki G, Segel MJ, Christensen TG, Conner MW, Breuer R. Time course of bleomycin-induced lung fibrosis. Int J Exp Pathol. 2002;83:111–9. https://doi.org/10.1046/j.1365-2613.2002.00220.x.
66. Hartl D, Griese M, Nicolai T, Zissel G, Prell C, Reinhardt D, et al. A role for MCP-1/CCR2 in interstitial lung disease in children. Respir Res. 2005;6:93. https://doi.org/10.1186/1465-9921-6-93.
67. Lis-López L, Bauset C, Seco-Cervera M, Cosín-Roger J. Is Macrophage Phenotype Determinant Fibros Development? Biomedicines. 2021;9. https://doi.org/10.3390/biomedicines9121747.
68. Patil RH, Naveen Kumar M, Kiran Kumar KM, Nagesh R, Kavya K, Babu RL, et al. Dexamethasone inhibits inflammatory response via down regulation of AP-1 transcription factor in human lung epithelial cells. Gene. 2018;645:85–94. https://doi.org/10.1016/j.gene.2017.12.024.
69. Rocksén D, Lilliehöök B, Larsson R, Johansson T, Bucht A. Differential anti-inflammatory and anti-oxidative effects of dexamethasone and N-acetylcysteine in endotoxin-induced lung inflammation. Clin Exp Immunol. 2000;122:249–56. https://doi.org/10.1046/j.1365-2249.2000.01373.x.
70. Vorobjeva NV, Chernyak BV, NETosis. Molecular mechanisms, Role in Physiology and Pathology. Biochem (Moscow). 2020;85:1178–90. https://doi.org/10.1134/S0006297920100065.
71. Yan S, Li M, Liu B, Ma Z, Yang Q. Neutrophil extracellular traps and pulmonary fibrosis: an update. J Inflamm. 2023;20:2. https://doi.org/10.1186/s12950-023-00329-y.
72. Nishida Y, Yagi H, Ota M, Tanaka A, Sato K, Inoue T et al. Oxidative stress induces MUC5AC expression through mitochondrial damage-dependent STING signaling in human bronchial epithelial cells. 2023; 5:171–81. https://doi.org/10.1096/fba.2022-00081.
73. Song JS, Kang CM, Yoo MB, Kim SJ, Yoon HK, Kim YK, et al. Nitric oxide induces MUC5AC mucin in respiratory epithelial cells through PKC and ERK dependent pathways. Respir Res. 2007;8:28. https://doi.org/10.1186/1465-9921-8-28.
74. Ballester B, Milara J, Cortijo J. Mucins as a New Frontier in Pulmonary Fibrosis. J Clin Med. 2019;8. https://doi.org/10.3390/jcm8091447.
75. Cunningham JT, Rodgers JT, Arlow DH, Vazquez F, Mootha VK, Puigserver P. mTOR controls mitochondrial oxidative function through a YY1-PGC-1alpha transcriptional complex. Nature. 2007;450:736–40. https://doi.org/10.1038/nature06322.
76. Rajapakse AG, Yepuri G, Carvas JM, Stein S, Matter CM, Scerri I, et al. Hyperactive S6K1 mediates oxidative stress and endothelial dysfunction in aging: inhibition by resveratrol. PLoS ONE. 2011;6:e19237. https://doi.org/10.1371/journal.pone.0019237.
77. Montuschi P, Ciabattoni G, Paredi P, Pantelidis P, du Bois RM, Kharitonov SA, et al. 8-Isoprostane as a biomarker of oxidative stress in interstitial lung diseases. Am J Respir Crit Care Med. 1998;158:1524–7. https://doi.org/10.1164/ajrccm.158.5.9803102.
78. Lakari E, Soini Y, Säily M, Koistinen P, Pääkkö P, Kinnula VL. Inducible nitric oxide synthase, but not xanthine oxidase, is highly expressed in interstitial pneumonias and granulomatous diseases of human lung. Am J Clin Pathol. 2002;117:132–42. https://doi.org/10.1309/w7t9-hw9v-v94b-r9km.
79. Li J-p, Gao Y, Chu S-f, Zhang Z, Xia C-y, Mou Z, et al. Nrf2 pathway activation contributes to anti-fibrosis effects of ginsenoside Rg1 in a rat model of alcohol- and CCl4-induced hepatic fibrosis. Acta Pharmacol Sin. 2014;35:1031–44. https://doi.org/10.1038/aps.2014.41.
80. Kong L, Deng J, Zhou X, Cai B, Zhang B, Chen X, et al. Sitagliptin activates the p62–Keap1–Nrf2 signalling pathway to alleviate oxidative stress and excessive autophagy in severe acute pancreatitis-related acute lung injury. Cell Death Dis. 2021;12:928. https://doi.org/10.1038/s41419-021-04227-0.
81. Iizuka T, Ishii Y, Itoh K, Kiwamoto T, Kimura T, Matsuno Y et al. Nrf2-deficient mice are highly susceptible to cigarette smoke-induced emphysema. 2005; 10:1113–25. https://doi.org/10.1111/j.1365-2443.2005.00905.x.
82. Ying Y-H, Lin X-P, Zhou H-b, Wu Y-f, Yan F-g, Hua W, et al. Nuclear erythroid 2 p45-related factor–2 Nrf2 ameliorates cigarette smoking-induced mucus overproduction in airway epithelium and mouse lungs. Microbes Infect. 2014;16:855–63. https://doi.org/10.1016/j.micinf.2014.08.014.
83. Jangam A, Tirunavalli SK, Adimoolam BM, Kasireddy B, Patnaik SS, Erukkambattu J, et al. Anti-inflammatory and antioxidant activities of Gymnema Sylvestre extract rescue acute respiratory distress syndrome in rats via modulating the NF-κB/MAPK pathway. Inflammopharmacology. 2023;31:823–44. https://doi.org/10.1007/s10787-022-01133-5.
84. Kaur R, Shaikh TB, Priya Sripadi H, Kuncha M, Vijaya Sarathi UVR, Kulhari H, et al. Nintedanib solid lipid nanoparticles improve oral bioavailability and ameliorate pulmonary fibrosis in vitro and in vivo models. Int J Pharm. 2024;649:123644. https://doi.org/10.1016/j.ijpharm.2023.123644.
85. Peng D, Fu M, Wang M, Wei Y, Wei X. Targeting TGF-β signal transduction for fibrosis and cancer therapy. Mol Cancer. 2022;21:104. https://doi.org/10.1186/s12943-022-01569-x.

Publisher's Note Springer Nature remains neutral with regard to jurisdictional claims in published maps and institutional affiliations.

Springer Nature or its licensor (e.g. a society or other partner) holds exclusive rights to this article under a publishing agreement with the author(s) or other rightsholder(s); author self-archiving of the accepted manuscript version of this article is solely governed by the terms of such publishing agreement and applicable law.